Regional Collagen Fiber Network in the Articular Disc of the Human Temporomandibular Joint: Biochemical 3-Tesla Quantitative Magnetic Resonance Imaging Compared to Quantitative Histologic Analysis of Fiber Arrangement

Jaryna Eder, DMD
Assistant Doctor
Department of Prosthodontics
University Clinic of Dentistry Vienna
Medical University of Vienna, Vienna, Austria

Zbynek Tonar, MD, PhD
Assistant Professor
Department of Histology and Embryology
Biomedical Center, Faculty of Medicine in Pilsen
Charles University, Pilsen, Czech Republic

Martina Schmid-Schwap, MD, DMD
Professor

Margit Bristela, MD, DMD, MSc
Senior Doctor

Astrid Skolka, MD, DMD, MSc
Senior Doctor

Department of Prosthodontics
University Clinic of Dentistry Vienna

Hannes Traxler, MD
Assistant Professor
Department of Anatomy

Eva Piehslinger, MD, DMD
Professor
Department of Prosthodontics
University Clinic of Dentistry Vienna

Medical University of Vienna
Vienna, Austria

Monika Egerbacher, DVM
Professor
Institute of Anatomy
Department of Pathobiology
University of Veterinary Medicine Vienna
Vienna, Austria

Siegfried Trattnig, MD
Professor
High Field MR Center
Department of Biomedical Imaging and Image-Guided Therapy
Medical University of Vienna;
CD Laboratory for Molecular Clinical MR Imaging;
Austrian Cluster for Tissue Regeneration
Ludwig Boltzmann Institute for Experimental and Clinical Traumatology, Vienna, Austria

Kirsti Witter, DVM, PhD
Assistant Professor
Institute of Anatomy
Department of Pathobiology
University of Veterinary Medicine Vienna
Vienna, Austria

Correspondence to:
Dr Jaryna Eder
Medical University of Vienna
Sensengasse 2a, 1090 Vienna, Austria
Fax: +431 40070-4909
Email: jaryna.eder@meduniwien.ac.at

Aims: To evaluate the regional collagen fiber network in the human temporomandibular joint (TMJ) disc by using biochemical magnetic resonance imaging (MRI) and quantitative histology. **Methods:** MRI of 5 heads (10 TMJ discs) obtained from partially dentate or edentulous cadavers was performed at 3-Tesla MRI by using a flexible, 8-channel transmit-receive coil. After MRI, all 10 discs were processed histologically. Percentages of coronal, sagittal, and transverse collagen fibers were assessed stereologically for the anterior, central, and posterior parts of the disc. An anisotropy index was calculated for collagen fiber arrangement in all three regions of interest. **Results:** In the central part of the TMJ disc, collagen fibers were arranged anisotropically with a preferentially sagittal direction. In the anterior and posterior parts, evidence for fibers being arranged isotropically (randomly) without preferred direction was found. Mean MRI T2 values appeared to be correlated with the anisotropy index of collagen fibers ($r = -0.45$; $P < .05$). When tested individually, T2 values of the isotropic anterior and posterior disc regions showed a partial but significant correlation with the anisotropy index of collagen fibers ($r = -0.54$; $P < .05$), whereas the anisotropic central part did not ($P > .05$). **Conclusion:** This study has provided the first systematic comparison of quantitative data on collagen fiber isotropy and anisotropy assessed in histologic sections with biochemical quantitative MRI for human TMJ fibrous cartilage. *J Oral Facial Pain Headache 2018;32:266–276. doi: 10.11607/ofph.1879*

Keywords: *comparison of MRI and histology, fibrocartilage, MRI, temporomandibular joint, 3 Tesla*

The human articular disc of the temporomandibular joint (TMJ) is located between the mandibular condyle and the glenoid fossa of the articular eminence of the temporal bone.[1,2] It mainly functions as a load absorber, makes relative motion possible, and undertakes tensile, compressive, and shear mechanical load from different directions during various motions such as chewing or talking.[3–8]

These functions are ensured by the shape and specific tissue composition of the TMJ disc. The disc is a flexible but firm plate, considerably thinner in the center than on its periphery, and shows a species-specific anatomical shape. The inferior surface of the disc is concave and fits on top of the rounded condyle. The anterior and posterior bands of the disc have thickened edges, the posterior band being distinctly thicker. In the sagittal plane, the disc is biconcave.[7,9–11]

The fibrocartilage of the human TMJ disc is made up of a few cells, collagen, proteoglycans, and water. It is an avascular, alymphatic, aneural tissue. Its main component is collagen type I,[6,12] and its nutrition depends mainly on diffusion of the synovial fluid.[13] The collagen fibers are structurally highly organized, forming a fine network that acts to entrap large proteoglycan aggregates in the extrafibrillar space.[13] Thus, the fibrous network plays an important role in reinforcement and mechanical stability of the joint. Due to the volume predominance of the collagen type I component, it can be expected that it would have an impact on the way that mechanical load is allocated in the disc.[11]

Characterization of the composition of the TMJ disc, especially of its fiber network, is necessary for a better understanding of temporomandibular disorders (TMD), TMJ anatomy and pathology, and for developing functional tissue replacements.[11,14] TMD are comparatively frequent, with 5% to 40% of the adult human population suffering from these complaints.[15–17] Many disorders of the TMJ result from disc dysfunction, with disc dislocation being one common clinical finding. It has been suggested that degenerative processes predispose the disc to displacement and result in significant changes in disc morphology, function, and material properties.[18,19]

Magnetic resonance imaging (MRI) is the only modality for direct noninvasive visualization of the articular cartilage and articular disc.[20,21] It thus allows noninvasive morphologic and biochemical assessment.[22,23] Numerous studies have shown the feasibility of using 3-Tesla (3T) MRI for morphologic imaging of small joints.[21,24–26] Moreover, several techniques have been developed that use MRI for the direct visualization of cartilage structure and molecular composition in vivo.[27–29] T2 maps allow quantitative evaluation of collagen fiber composition and its orientation properties. It is assumed that the orientation of collagen fibers influences mobility of water molecules.[20,30–33] T2 relaxation time, also referred to as spin-spin relaxation time, is related to the interaction of spins of protons in water molecules. T2 mapping with a high–field strength MRI scanner allows for structural analysis of the TMJ disc composition on a near-microscopic level.[24,25]

Although MRI is used for diagnosis and experimental imaging approaches of the TMJ disc and its diseases, it is still largely unknown which structural changes of the disc that can be observed in MRI scans underlie changes in T2 weight values. It has been claimed that regional variations in collagen fiber orientation can be determined through the T2 heterogeneity of cartilage.[31,32] However, no direct correlation between histologic and MRI findings has yet been established for the fibrocartilaginous disc of the TMJ.

The aim of this study was to evaluate the regional collagen fiber network in the human TMJ disc by using biochemical MRI and quantitative histology. Three regions of interest (ROIs) of the disc were examined by MRI as well as by quantitative histology, with special emphasis on the distribution and arrangement of the collagen fiber network. This study addressed the following questions: *(1)* Are collagen fibers arranged isotropically in ROIs of the human TMJ disc? *(2)* Are MRI T2 values correlated with the percentage of collagen fibers running in the sagittal direction; ie, the MRI section plane? and *(3)* Are MRI T2 values correlated with the measure of collagen fiber anisotropy in the respective ROI?

Materials and Methods

Specimens

Human cadavers were provided by the Center of Anatomy and Cell Biology of the Medical University of Vienna. The approval of the ethics committee was obtained before the examination. Five heads were obtained from partially dentate or edentulous cadavers (mean ± standard deviation [SD] age 74.5 ± 5.5 years; two females, three males). Available information did not contain anything about history of TMD. The cadavers were stored at –20°C and defrosted carefully for the study. After the MRI examination, the TMJs were harvested en bloc and immersed in Histofix (Carl Roth) for transport (maximal storage time 1 hour). Afterwards, the discs (n = 10) were carefully removed and fixed definitively in buffered formalin according to Lillie.[34]

Nomenclature of Planes and Directions

Section planes for virtual sectioning in MRI and sampling for histology were chosen according to Scapino et al.[12] For the sake of readability in this article, however, the terms coronal, sagittal, and transverse for designation of planes and directions, as given in Table 1, are used.

Magnetic Resonance Imaging

MRI Examination. MRI was performed on a 3T MRI scanner (Magnetom TIM Trio, Siemens Healthcare) using a flexible, dedicated, 8-channel multi-element transmit-receive coil (Noras). Human heads were placed into the MRI coil. Coil elements were in close contact with the heads, which guaranteed optimal MRI signal reception. Heads were sealed in plastic bags. Right and left joints were imaged simultaneously in closed position, covering 6 slices on both sides (12 slices in total). Slices were oriented oblique sagittal in morphologic as well as in T2 multi-slice multi-echo Carr-Purcell-Meiboom-Gill (CPMG) protocols. CPMG is a widely used method for T2 mapping that yields signals from several time points (echoes) along the T2 decay. The most important sequence parameters for T2 mapping using CPMG were as follows: repetition time (TR) was set to 1,440 milliseconds, and 10 echoes were acquired with minimum echo time (TE) of 11.2 milliseconds and maximum echo time of 112 milliseconds. Field of view was set to 155 × 155 mm and matrix size was 384 × 384 pixels, corresponding to the nominal in-plane resolution of 0.4 × 0.4 mm. Time of acquisition was 14 minutes, 47 seconds. Additional parameters are listed in Table 2. The resulting series of T2-weighted images were subsequently postprocessed into T2 maps by using built-in Siemens SYNGO software. A mono-exponential fitting procedure was performed

Table 1 Description of Anatomical Terminology for Section Planes and Directions Used in This Study for the TMJ Disc

Terms according to Scapino et al[12]	Description of section plane/anatomical direction	Term used in this article
IZ plane	Approximately parallel to the surfaces of the intermediate zone of the disc (ROI B)	Transverse
S plane	Perpendicular to the tangent of the superior disc surface when the disc is viewed from behind, between the condylar poles	Sagittal
ML plane	Perpendicular to the tangent of the superior surface of the IZ (viewed laterally) and parallel to the condylar long axis (viewed from above)	Coronal

Table 2 Magnetic Resonance Measurement Parameters for Car-Purcell-Meiboom-Gill Sequence (CPMG), Proton Density (PD), and Morphologic Double-Echo Steady-State Protocol (DESS)

	CPMG Sagittal (closed position)	DESS Coronal	PD Sagittal (opened position)
Field of view (mm × mm)	155 × 155	200 × 200	90 × 90
No. of slices (left + right)	6 + 6	256	11 + 11
Slice thickness (mm)	2	0.56	2
Slice separation (mm)	2.2	–	2.2
No. of averages	1	1	1
TR (ms)	1,440	15.16	1,810
TE (ms)	11.2 – 112.0	4.37	30
Echo train	10	1	1
Total acquisition time (min: sec)	14:47	9:49	4:56
Acquisition matrix (pixel)	384 × 384	358 × 448	384 × 384
Percent phase field of view	100	100	100
Percent sampling	100	80	100
Pixel bandwidth (Hz/pixel)	200	169	161
Magnetic resonance acquisition type	2D	3D	2D
Reconstructed matrix (pixel)	384 × 384	716 × 896	768 × 768
Pixel spacing (mm)	0.40 × 0.40	0.28 × 0.22	0.12 × 0.12

TR = repetition time; TE = echo time.

on all MRI data sets on a pixel-by-pixel basis. A three-parametric function was used to fit the signal intensity of images as a function of the TE. The following equation was used for fitting:

$$Si = A0 + A1 * \exp(-TE/A2)$$

. . . where Si is measured signal intensity and TE is echo time chosen for an MRI acquisition. Variables A0, A1, and A2 are unknown and must be estimated by the iterative process. A0 is baseline (dominantly comprising the noise), A1 corresponds to the proton density of the sample, and A2 corresponds to the actual T2 (mono-exponentially calculated T2) component.

Image Analysis. The image analysis was performed independently by three specialized and experienced examiners blinded to the identity of the cadavers. The examiners assessed images of the mouth in closed position according to the perceptibility of position/delineation to the surrounding tissue and morphology of the disc, as well as changes in signal and morphology of the disc. The location and positioning of the TMJ structures (condyle and disc) were evaluated on sagittal and coronal slices. The morphologic assessment and the selection of the ROIs were analogous to Schmid-Schwap et al[25] (Fig 1). Examiners drew the contours and the anterior (ROI A), central (ROI B), and posterior (ROI C) parts (for comparison with histology, see Fig 2) of the disc on the image with the best morphologic contrast and transferred it via copy and paste into the T2 map. In addition to ROIs A, B, and C, the whole-section image of the disc was analyzed (ROI whole disc). The whole project was supervised by a radiologist with 20 years of experience. Cadavers were numbered according to the internal evidence system of the Institute (heads 7 to 11).

Histologic Study

The TMJ discs were fixed in buffered formalin according to Lillie.[34] After fixation, they were divided midsagittally into lateral and medial parts. The lateral halves of the disc were stored as retained samples. The medial halves were processed as follows:

A sagittal slice of the discs was cut adjacent to the plane of division and embedded routinely in paraffin wax for cutting sagittal histologic sections,

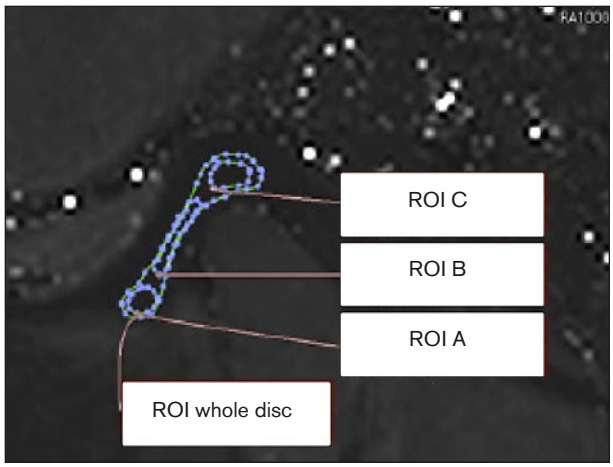

Fig 1 *(left)* Magnetic resonance imaging of the human TMJ disc (mouth closed) in sagittal section. Example of a T2 map. Regions of interest (ROIs A, B, and C representing anterior, central, and posterior parts of the disc, respectively) delineated in blue.

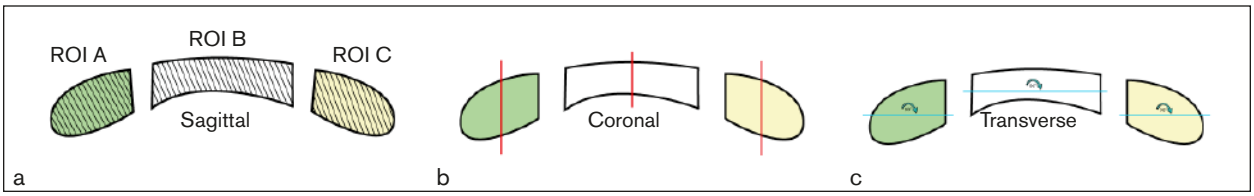

Fig 2 *(below)* Sampling of the human TMJ disc for histologic processing. The schematic drawing shows the sagittal section profile after dividing the disc into medial and lateral halves. Regions of interest (ROI): ROI A *(green)* = anterior part; ROI B *(white)* = central part; and ROI C *(yellow)* = posterior part. The gray lines **(a)** indicate the section profile of sagittal histologic sections (section plane 1), the red lines **(b)** the section plane of coronal sections (section plane 2), and the blue lines **(c)** the section plane of transverse sections (section plane 3).

showing ROIs A, B, and C in one section (section plane 1). The ROIs were defined for further qualitative and quantitative assessment as described for MRI image analysis; the rest of the medial disc halves were divided into three ROIs: ROI A (anterior part), ROI B (central part), and ROI C (posterior part). Out of the center of each of these tissue samples, two immediately adjacent coronal slices were taken. One of them was embedded for cutting coronal sections (section plane 2) and the other for transverse sections (section plane 3; Table 1 and Fig 2).

Sections were prepared at a thickness of 4 µm and mounted on APES-glutaraldehyde–coated slides (Sigma-Aldrich). Selected sagittal sections of all three ROIs were stained with hematoxylin and eosin (H&E) for analysis of the general histologic structure of the discs, with alcian blue (pH 2.5) for detection of glycosaminoglycans of the cartilaginous matrix and with picrosirius red in order to highlight the collagen fibers. H&E and alcian blue staining was performed according to Romeis and Böck.[34] The sections were analyzed by light microscopy. For picrosirius red staining, dewaxed and hydrated sections were stained with Weigert's hematoxylin for 8 minutes, followed by washing, then staining with picrosirius red (0.5 g Siriusred Direct red 80, Cat#365548, Sigma Aldrich) solved in a saturated aqueous solution of picric acid 1.3% in water (Sigma, Cat# P6744-1GA) for 1 hour. After they were washed and the water physically removed, the slides were dehydrated in 100% ethanol, cleared in xylene, and mounted in a resinous medium. These sections were analyzed by polarized light microscopy (linear polarization).

Furthermore, at least two sections per ROI and cutting plane were stained according to van Gieson.[34] For quantitative analysis, 10 micrographs were taken in a systematic, uniform, and random manner from at least two histologic sections representing each ROI and each orientation of the cutting plane. In total, a profile area of 8.04 mm^2 was analyzed per section (area of one micrograph at ×10 objective magnification was 0.804 mm^2). The objective magnification used (×10) guaranteed reliable visual control of all the fiber bundles. The variability among the microscopic image fields sampled from the sections was assessed in a pilot study (results not shown). Using the cumulative moving average, the pilot study performed in 9 human disc samples (ie, 90 micrographs) showed that 6 microscopic image fields per ROI and orientation provided a good estimate of the whole area of the sections. However, 10 image fields per tissue block were sampled to make sure that any accidental inhomogeneity would not bias the study. For the main study, a total of 890 micrographs were analyzed by one examiner (J.E.), representing three orientations (1, 2, 3) in each of the three ROIs (A, B, C) in 10 discs. The A1 sample from the right disc of no. 11 was excluded from the study since no tissue from this ROI was available.

In order to assess collagen fiber anisotropy in the TMJ disc, collagen fiber bundles running parallel to the histologic section plane (PCP fibers) were analyzed. The area of PCP fibers per area of the section profile was assessed using a stereologic point-counting technique for each ROI and section plane. A stereologic point grid (PointGrid module of the Ellipse

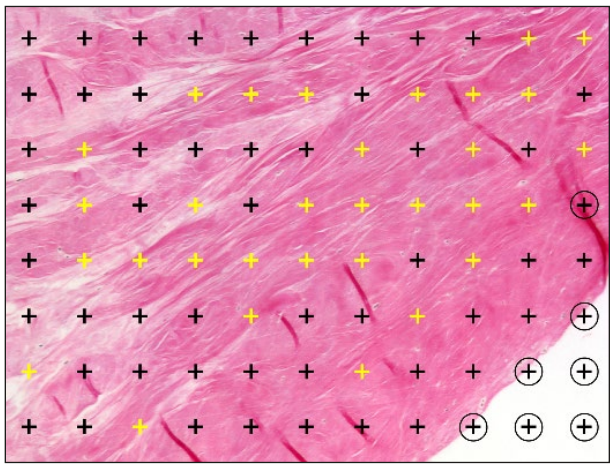

Fig 3 Assessment of areas of histologic sections covered with structures of interest by using a stereologic point grid. Micrograph of a human TMJ disc (staining van Gieson, objective magnification ×10, total area 0.804 mm²) superposed with a point grid containing 88 points. The area assigned to each point was 8,870 µm². Points hitting collagen fiber bundles running parallel to the histologic section plane (PCP fibers) were counted *(yellow crosses)*. Points hitting the profile of the TMJ disc were counted as reference value *(yellow crosses + black crosses)*. Areas not covered with tissue *(crosses with circles in lower right corner)* or areas covered with artifacts *(cross with circle on right side of micrograph)* were excluded from the reference area by not counting the corresponding points.

software, ViDiTo) was loaded and randomly superposed on the micrographs. According to the Delesse principle,[35] the area fraction of PCP fibers within the sectional area of the disc is consistent with the volume fraction of the PCP fibers within the disc. Both area and volume fraction are equal to the ratio:

$$\frac{\Sigma P_i(PCP\ fibers)}{\Sigma P_i\ (disc)}$$

. . . where P_i(PCP fibers) denotes the number of points of a stereologic grid hitting the PCP fibers in a micrograph, and P_i(disc) denotes the number of points of the same grid hitting the section profile of the disc. This resulted in the area fraction of PCP fibers within the disc, labeled A_A(PCP fibers, disc) from now on. The density of the point grid was chosen in accordance with the pilot study mentioned above so that the area corresponding to each point ($\frac{a}{p}$) was 8,870 µm² (Fig 3). This resulted in counting at least 200 points per ROI and cutting direction.[36]

Establishing Anisotropy of Collagen Fibers (Anisotropy Index)

The ratios A_A(PCP fibers, disc) for section planes 1, 2, and 3 were compared separately for each ROI. If these ratios were the same for all three section planes, isotropic arrangement of fibers was assumed. If the ratio was higher in two and lower in the third section plane, fibers were assumed to be arranged preferentially in one direction (anisotropically).

For further analysis and graphic presentation of the results, one single measure representing the degree of anisotropy was desirable. Mathematically correct models of spatial anisotropy, however, are based on analysis of definable individual oblong structures in three-dimensional (3D) space.[37–39] For collagen fibers within fibrous cartilage, this approach is technically not possible. On the level of light microscopy, individual collagen fibers and their endpoints cannot be identified. The 3D approach would moreover require identification of these fibrous structures either in thick sections or in precise serial sections that can be registered for 3D reconstruction. Another limitation for the use of established measures of anisotropy is that they have to be expressed as matrices (eg, 3 × 3 matrices for ellipsoidal anisotropy). This form of data presentation impedes further analysis with standard statistical methods.

Therefore, an easy, one-dimensional parameter for collagen fiber anisotropy in the TMJ disc that allows comparison between samples and correlation with MRI data was established. Based on the A_A(PCP fibers, disc) ratios for the section planes 1, 2, and 3, it was proceeded as follows: The geometric mean of the three A_A(PCP fibers, disc) ratios was calculated. In its geometrical interpretation, the geometric mean represents the edge length x of a cube with the same volume as a rectangular cuboid with the edge lengths A_A(PCP fibers, disc)1, A_A(PCP fibers, disc)2, and A_A(PCP fibers, disc)3. If collagen fibers were arranged isotropically, A_A(PCP fibers, disc) would be equal in all three section planes and the geometric mean the same as the single A_A(PCP fibers, disc) values. In the case of anisotropic fiber arrangement, differences from x can be calculated for A_A(PCP fibers, disc) in all three section planes: $a = |A_A(\text{PCP fibers, disc})1\text{-}x|$, $b = |A_A(\text{PCP fibers, disc})2\text{-}x|$, and $c = |A_A(\text{PCP fibers, disc})3\text{-}x|$. In order to obtain a single value (anisotropy index) that can be used as an equivalent to established anisotropy measures for further data analysis, a, b, and c were summed. A large anisotropy index signifies that in at least one section plane the A_A(PCP fibers, disc) value differs considerably from the ideal a = b = c = x, as would be calculated in case of isotropic fiber distribution. An anisotropy index of 0 signifies isotropy.

Statistical Analyses

Friedman test with post hoc Wilcoxon matched pair test were used to compare A_A(PCP fibers, disc) values found in different section planes in the re-

Fig 4 *(right)* Mean ± standard deviation T2 values for the different regions of interest (ROIs) and different raters. The central part (ROI B) of the disc had the tendency to show the lowest T2 values.

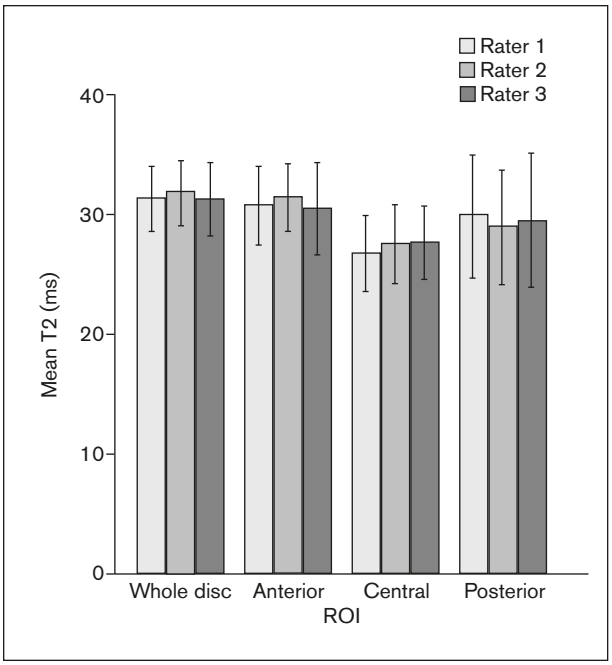

Table 3 Morphologic Assessment of Magnetic Resonance Images of the Human TMJ Disc

Cadaver head/side	Condyle	Disc position	Arthritis
7			
Right	Distraction	Normal	No
Left	Retral	Normal	Little
8			
Right	Distraction	Partial dislocation	Little
Left	Distraction	Partial dislocation	Little
9			
Right	Normal	Partial dislocation	Distinct
Left	Normal	Partial dislocation	No
10			
Right	Normal	Normal	No
Left	Distraction	Normal	No
11			
Right	Distraction	Normal	No
Left	Distraction	Normal	No

Table 4 MRI of the TMJ T2 Values in All Individual Discs in Their Respective Anterior, Central, and Posterior Parts (ROIs A, B, and C, Respectively)

	Right side (ms)		Left side (ms)	
Discs/ROI	Mean T2	SD	Mean T2	SD
7				
A	26.960	0.106	32.393	0.564
B	22.021	1.308	25.300	1.267
C	43.532	2.451	30.874	0.795
8				
A	34.350	1.252	36.589	0.947
B	25.724	0.545	30.924	1.095
C	27.608	0.055	34.727	0.578
9				
A	33.644	1.140	36.274	0.034
B	21.789	1.259	27.242	0.321
C	22.424	1.313	26.617	1.934
10				
A	23.383	4.315	25.345	0.626
B	27.149	4.488	26.173	0.489
C	20.118	0.783	24.369	0.103
11				
A	Missing		30.602	0.803
B	31.954	0.718	35.073	0.395
C	28.280	2.067	37.128	1.395

ROI = region of interest; SD = standard deviation; MRI = magnetic resonance imaging.

spective ROIs belonging to one disc. The Kruskal-Wallis analysis of variance (ANOVA) test was used to assess the differences between the A_A(PCP fibers, disc) values resulting from the image fields acquired in different cutting plane orientations in every ROI for each disc separately. Rater agreement was calculated using intraclass correlation coefficient (ICC). In order to assess associations between T2 values and PCP fibers, as well as between T2 values and anisotropy index, Pearson linear correlation coefficient was used. All tests were used as available in the Statistica Base 11 package (StatSoft). A value of $P \leq .05$ was considered to indicate significant results.

Results

Morphologic Assessment by MRI

The morphologic assessment was conducted as described by Schmid-Schwap et al.[25] Its results are summarized in Table 3. Although several moderate alterations were found, neither significant effusion nor disc disruption were detected.

Biochemical Analysis (MRI T2 TR Mapping)

The mean ± SD T2 values for the human TMJ disc were 31.5 ± 1.6 milliseconds, 30.9 ± 2.0 milliseconds, 27.3 ± 1.7 milliseconds, and 29.5 ± 2.8 milliseconds for the whole disc, ROI A, ROI B, and ROI C, respectively. T2 values for all ROIs in each disc can be found in Table 4. The ICC for intraclass variability was 0.926. This shows very good agreement between the observers. The results of all ROIs and raters are summarized in *Fig* 4. Repeated measures ANOVA revealed no significant differences between the raters ($P = .757$). There were no significant differences between the T2 values in the ROIs A, B, and

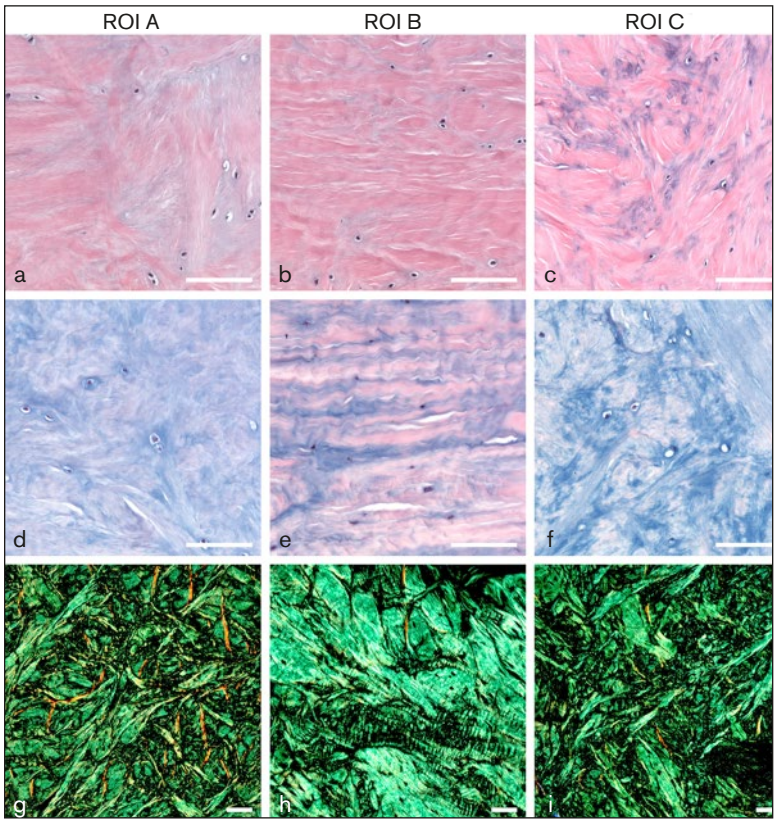

Fig 5 Microstructure of the human TMJ disc in region of interest (ROI) A (anterior part of the disc), ROI B (central part), and ROI C (posterior part). **(a–c)** Hematoxylin and eosin staining. **(d–f)** Alcian blue staining (pH 2.5). **(g–i)** Picrosirius red staining and polarized light microscopy. Note the lower cartilage matrix content (a–c: purple; d–f: blue) in ROI B in contrast to ROIs A and C and the preferentially sagittal orientation of collagen fiber bundles in ROI B. Sagittal section plane. Scale bar: 100 µm.

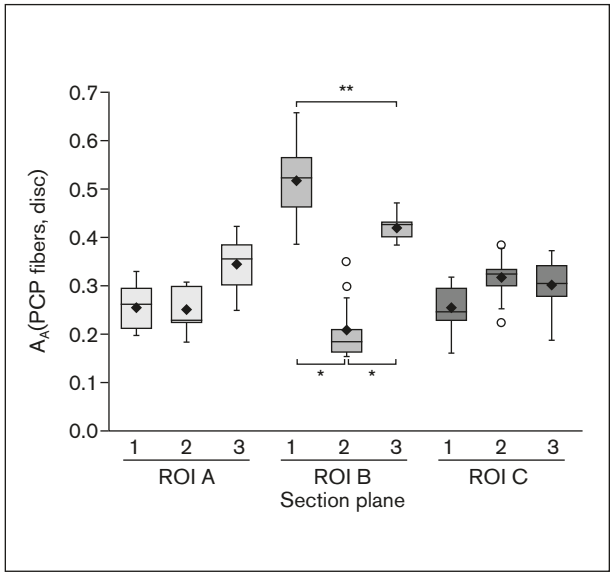

Fig 6 Area fractions of collagen fiber bundles running parallel to the histologic section plane (PCP fibers) within the TMJ disc (A_A[PCP fibers, disc]) in three regions of interest (ROI A, anterior part; ROI B, central part; ROI C, posterior part) and three histologic section planes (1, sagittal; 2, coronal; 3, transverse). The Friedman ANOVA showed significant differences among the orientations within ROI B only ($P < .001$). The significant P values for the post hoc Wilcoxon matched pairs test between B1, B2, and B3 are presented. *$P = .0051$. **$P = .0093$. Data are displayed as median values with boxes spanning the upper limits of the first and third quartiles and with whiskers spanning the minimum and maximum values for each group. Mean values are depicted as black diamonds and outliers as circles.

C ($P = .361$). However, the T2 values of ROI B of the disc tended to be the lowest.

Histologic Analysis

The microstructure of the human TMJ disc in ROIs A, B, and C is shown in Fig 5. The fibrous cartilage of ROI A and C consisted of collagen fiber bundles arranged in all directions of space and a higher glycosaminoglycan content compared to ROI B. Collagen fibers in ROI B seemed to run preferentially sagittally.

In order to test whether collagen fibers were indeed arranged isotropically in ROIs A and C and anisotropically (ie, with a preferred direction) in ROI B, A_A(PCP fibers, disc) ratios of section planes 1, 2, and 3 were compared to each other for each ROI. The comparison of the pooled mean data (Fig 6) revealed a statistically significant difference ($P = .001$) between the sagittal section plane compared to the coronal and transverse planes in ROI B. In this region, the area fraction of PCP fibers was largest in section plane 1 (sagittal), followed by section plane 3. The lowest values were in the sections with section plane 2. This means that the collagen fibers were arranged anisotropically with a preferentially sagittal direction. No significant differences between section planes could be found for ROI A or for ROI C ($P = .121$ and $P = .061$, respectively); ie, in ROIs A and C, the fibers were arranged isotropically (randomly) without a preferred direction.

The Kruskal-Wallis test was used to compare the ROIs of each disc individually. In all discs, the A_A(PCP fibers, disc) of the sagittal section plane of ROI B differed significantly from the coronal and transverse section planes. In some discs, fibers in ROIs A and C were arranged anisotropically (Table 5).

Correlation of the T2 Values with Sagittal Collagen Fibers

There was no significant general correlation of the T2 values with the area fraction of sagittal collagen fibers within the TMJ disc ($P > .05$). However, when potentially isotropic ROIs (ROI A and ROI C) and anisotropic ROI B were tested individually, the area fraction of sagittal collagen fibers in the margins of the discs (ROI A and ROI C) correlated significantly ($r = -0.54$; $P < .05$) with T2 values, as shown in Fig 7. No correlation was found for the central part (ROI B) of the disc ($P > .05$).

Correlation of the T2 Values with the Anisotropy Index

The mean T2 values were correlated with the anisotropy index based on the A_A(PCP fibers, disc) ratios for section planes 1, 2, and 3 ($r = -0.45$; $P < .05$) (Fig 8). Potentially isotropic ROIs (ROI A and ROI C) and anisotropic ROI B were also tested individually. T2 values of ROI A and ROI C showed a significant correlation with the anisotropy index ($r = -0.54$; $P < .05$), whereas the central part (ROI B) did not ($P > .05$).

Discussion

Characterization of the composition of the TMJ disc, especially of its fiber network, is necessary for a better understanding of TMD, TMJ anatomy, and pathology, as well as for developing functional tissue replacements. This study has provided the first systematic comparison of quantitative data on collagen fiber isotropy and anisotropy assessed in histologic sections with biochemical quantitative MRI for human fibrous cartilage.

Qualitative examination of histologic sections of the human TMJ disc by light and polarization microscopy provided profile images corresponding to the 3D fiber architecture as described in detail by Scapino et al.[12] In the anterior and posterior disc regions (ROIs A and C, respectively), a meshwork of collagen fibers filled with glycosaminoglycans could be found. The water binding glycosaminoglycans can be expected to contribute to MR signal changes,[40] although a number of authors have shown that glycosaminoglycans and their bound water play only a minor role in T2 signal generation.[41–43]

Table 5 Comparison of Area Fractions of Collagen Fiber Bundles Running in Parallel to the Histologic Section Plane (PCP Fibers) for Individual TMJ Discs

Kruskal-Wallis ANOVA	A1 vs A2 vs A3	B1 vs B2 vs B3	C1 vs C2 vs C3
Disc 7 right	**.005**	**< .001**	NS
Disc 7 left	NS	**< .001**	NS
Disc 8 right	NS	**< .001**	NS
Disc 8 left	**.016**	**< .001**	**.014**
Disc 9 right	**< .001**	**< .001**	NS
Disc 9 left	NS	**< .001**	NS
Disc 10 right	**< .001**	**.041**	**< .001**
Disc 10 left	**< .001**	**< .001**	**.001**
Disc 11 right[a]	ND	**< .001**	**.008**
Disc 11 left	**.011**	**.002**	NS

P values of the Kruskal-Wallis ANOVA show the detailed differences between A_A(PCP fibers, disc) ratios quantified in histologic image fields taken from three section planes (1, 2, 3) per region of interest (ROI A, B, C). NS = not significant; ND = not defined. Significant values are in bold.
[a]A1 missing.

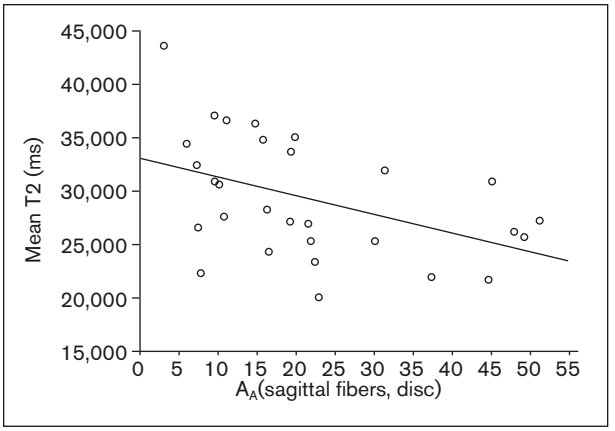

Fig 7 Pearson correlation of the mean MRI T2 values with the area fraction of sagittal collagen fiber bundles within the human TMJ disc (A_A[sagittal fibers, disc]) in its anterior and posterior parts. Significant correlation ($r = -0.54$; $P < .05$).

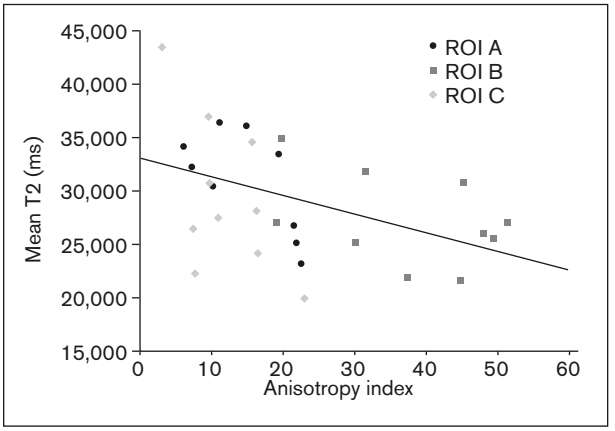

Fig 8 Pearson correlation of the mean MRI T2 values with the index of collagen fiber anisotropy (0 = isotropically arranged collagen fibers; higher values = higher degree of anisotropy) in the human TMJ disc. Significant correlation ($r = -0.45$; $P < .05$).

Until now, collagen fiber arrangement has been quantified in histologic sections mostly by birefringency index assessed by polarized light microscopy.[2,12] In order to include all fibers of the respective histologic section, circular polarization would be required. In this analysis, another technique but a similar approach to depict collagen fiber isotropy or anisotropy quantitatively was used based on comparison of the percentage of PCP fibers in three orthogonal section planes, and an easy anisotropy index calculated from these values. In contrast to "true" anisotropy measures,[37] the simplified anisotropy index can be applied on unregistered, thin histologic sections. Quantitative data on collagen fiber arrangement assessed by this approach correspond well to the qualitative findings: In the central part of the disc (ROI B), nearly 50% of the fibers run sagittally, whereas in the anterior and posterior parts of the disc (ROIs A and C), approximately 20% to 35% (ie, roughly one third) of the fibers run in each of the three section planes, signifying a nearly isotropic fiber arrangement. The lowest anisotropy indexes (ie, nearly ideal isotropic fiber distribution) were reached in some discs in ROIs A and C.

Despite this general pattern of anisotropic central and isotropic marginal regions of the human TMJ disc, anisotropic fiber arrangement in ROIs A and C in single discs were observed. Some of these showed partial disc dislocation. This appears to indicate that fibers show different results on account of the dislocation having altered mechanical pressure conditions. So where ROIs A or C do not display isotropic fiber arrangement, a connection with disc position might exist.

A moderate negative correlation between PCP fibers in sagittal histologic sections or anisotropy index on one side and T2 values on the other side was detected in the present study. It must still be established whether the higher glycosaminoglycan/water content within the isotropic 3D fiber network provides the explanation for the higher T2 values in ROIs A and C of the TMJ disc, as discussed above. If so, the lack of correlation between fiber (an)isotropy and T2 values in ROI B is surprising.

Another possible explanation for the differing T2 values lies in the collagen fiber distribution itself. For hyaline cartilage, it was established that T2 maxima are dependent on the quantity of collagen fibers that are arranged in a specific angle in reference to the static field.[26,41,44] The same might apply also for fibrous cartilage. In isotropic regions of the TMJ disc (ROIs A and C), there would be a higher probability of some fibers running in the "correct" direction, thus generating higher T2 values. In contrast, the anisotropic central ROI B might generate high or low T2 values depending on the angle between preferred (sagittal) fiber orientation and static field. Regarding the complex 3D structure of the human TMJ and its irregularly shaped disc, it is very well possible that the respective mutual orientation of ROI B and the MRI field differed between the heads under study so that no unequivocal correlation between collagen fiber arrangement and MR T2 values could be found in this region. As the correlation coefficients are between 0.45 and 0.54, (only) approximately 20% to 30% of T2 changes might be caused by fiber arrangement. Further studies are needed to investigate the remaining parameters.

A second item that has to be taken into account for assessment of correlations between MRI results and structure of the disc in ROI B is its very narrow profile area. Only a few pixels of the MR images are therefore included in the mean T2 readouts, so that single outliers could change the results considerably. Surrounding pixels might influence the readouts in this small zone as well. Marik et al[22] highlighted in their study that it is challenging to evaluate small joints with high curvature with an MRI. A certain minimal size and a certain outline seem to be needed for a meaningful evaluation. This could open a new field of quantitative tissue analysis, where advantages of T2 as a biomarker could lead to better monitoring of tissue changes due to disease as well as tissue response to different therapy approaches.

Some limitations of a cadaver study when applied to living patients have to be taken into account. The population examined for this study contained mostly elderly persons, in whom certain degenerative changes might have occurred due to age without clinical signs. However, it has been reported that collagen type I content and distribution do not differ between the age groups 30 to 39 years and 60 to 69 years.[7] On the other hand, ongoing decomposition processes due to storage of the cadavers might potentially influence results of MRI as well as of histologic examination. Control imaging of living patients and collection of fresh tissue samples would therefore be desirable.

Previous studies on similar topics have used animal models, whereas interspecies differences have to be underlined as an important caveat. According to Kalpacki et al,[45] it can be noted that if animal models are used for TMJ bioengineering efforts, pig discs should be preferred since they are most similar to human discs.

Conclusions

This study indicated that in the central part of the TMJ disc, collagen fibers are arranged anisotropically with a preferentially sagittal direction. In the anterior and posterior parts, evidence for fibers being arranged

isotropically (randomly) without preferred direction was found. Mean MRI T2 values appeared to be correlated with the anisotropy index of collagen fibers ($r = -0.45$; $P < .05$). When tested individually, T2 values of the isotropic anterior and posterior disc regions showed partial but significant correlation with the anisotropy index of collagen fibers ($r = -0.54$; $P < .05$), whereas the anisotropic central part did not ($P > .05$). Further research supporting the connection between collagen fiber arrangement and MRI may be necessary.

Acknowledgments

The financial support by the Austrian Federal Ministry of Science, Research, and Economy and the National Foundation for Research, Technology and Development is gratefully acknowledged. Zbynek Tonar received support from the Austrian Agency for International Mobility and Cooperation in Education, Science, and Research (ÖeAD) and from the Q39 Project of the Charles University Research Fund. The authors thank Claudia Kronnewetter (High Field MR Center of Excellence, Medical University of Vienna) and Sonja Walzer (Ortholab-AKH, Medical University of Vienna) for their support and Magdalena Helmreich, Anne Flemming, and Brigitte Machac (University of Veterinary Medicine Vienna) for their excellent technical assistance during the preparation of histologic sections. The authors report no conflicts of interest.

References

1. Werner JA, Tillmann B, Schleicher A. Functional anatomy of the temporomandibular joint. A morphologic study on human autopsy material. Anat Embryol (Berl) 1991;183:89–95.
2. Minarelli AM, Del Santo Júnior M, Liberti EA. The structure of the human temporomandibular joint disc: A scanning electron microscopy study. J Orofac Pain 1997;11:95–100.
3. Mills DK, Fiandaca DJ, Scapino RP. Morphologic, microscopic, and immunohistochemical investigations into the function of the primate TMJ disc. J Orofac Pain 1994;8:136–154.
4. Scapino RP, Canham PB, Finlay HM, Mills DK. The behaviour of collagen fibres in stress relaxation and stress distribution in the jaw-joint disc of rabbits. Arch Oral Biol 1996;41:1039–1052.
5. Beatty MW, Bruno MJ, Iwasaki LR, Nickel JC. Strain rate dependent orthotropic properties of pristine and impulsively loaded porcine temporomandibular joint disk. J Biomed Mater Res 2001;57:25–34.
6. de Bont LG, Liem RS, Havinga P, Boering G. Fibrous component of the temporomandibular joint disk. Cranio 1985;3: 368–373.
7. Minarelli AM, Liberti EA. A microscopic survey of the human temporomandibular joint disc. J Oral Rehabil 1997;24:835–840.
8. Shengyi T, Xu Y. Biomechanical properties and collagen fiber orientation of TMJ discs in dogs: Part 1. Gross anatomy and collagen fiber orientation of the discs. J Craniomandib Disord 1991;5:28–34.
9. Katzberg RW, Tallents RH. Normal and abnormal temporomandibular joint disc and posterior attachment as depicted by magnetic resonance imaging in symptomatic and asymptomatic subjects. J Oral Maxillofac Surg 2005;63:1155–1161.
10. Hansson LG, Westesson PL, Katzberg RW, et al. MR imaging of the temporomandibular joint: Comparison of images of autopsy specimens made at 0.3 T and 1.5 T with anatomic cryosections. AJR Am J Roentgenol 1989;152:1241–1244.
11. Allen KD, Athanasiou KA. Tissue engineering of the TMJ disc: A review. Tissue Eng 2006;12:1183–1196.
12. Scapino RP, Obrez A, Greising D. Organization and function of the collagen fiber system in the human temporomandibular joint disk and its attachments. Cells Tissues Organs 2006;182:201–225.
13. Jackson A, Gu W. Transport properties of cartilaginous tissues. Curr Rheumatol Rev 2009;5:40.
14. Murphy MK, Arzi B, Hu JC, Athanasiou KA. Tensile characterization of porcine temporomandibular joint disc attachments. J Dent Res 2013;92:753–758.
15. Hansson T, Nilner M. A study of the occurrence of symptoms of disease of the temporomandibular joint masticatory musculature and related structures. J Oral Rehabil 1975;2:313–324.
16. Dworkin SF, Huggins KH, LeResche L, et al. Epidemiology of signs and symptoms in temporomandibular disorders: Clinical signs in cases and controls. J Am Dent Assoc 1990;120:273–281.
17. Reston JT, Turkelson CM. Meta-analysis of surgical treatments for temporomandibular articular disorders: A reply to the discussants. J Oral Maxillofac Surg 2003;61:737–738.
18. Almarza AJ, Athanasiou KA. Evaluation of three growth factors in combinations of two for temporomandibular joint disc tissue engineering. Arch Oral Biol 2006;51:215–221.
19. Stegenga B. Osteoarthritis of the temporomandibular joint organ and its relationship to disc displacement. J Orofac Pain 2001;15:193–205.
20. Trattnig S, Mlynárik V, Huber M, Ba-Ssalamah A, Puig S, Imhof H. Magnetic resonance imaging of articular cartilage and evaluation of cartilage disease. Invest Radiol 2000;35:595–601.
21. Stehling C, Vieth V, Bachmann R, et al. High-resolution magnetic resonance imaging of the temporomandibular joint: Image quality at 1.5 and 3.0 Tesla in volunteers. Invest Radiol 2007; 42:428–434.
22. Marik W, Apprich S, Welsch GH, Mamisch TC, Trattnig S. Biochemical evaluation of articular cartilage in patients with osteochondrosis dissecans by means of quantitative T2- and T2-mapping at 3T MRI: A feasibility study. Eur J Radiol 2012; 81:923–927.
23. Quirbach S, Trattnig S, Marlovits S, et al. Initial results of in vivo high-resolution morphological and biochemical cartilage imaging of patients after matrix-associated autologous chondrocyte transplantation (MACT) of the ankle. Skeletal Radiol 2009;38:751–760.
24. Schmid-Schwap M, Drahanowsky W, Bristela M, Kundi M, Piehslinger E, Robinson S. Diagnosis of temporomandibular dysfunction syndrome—Image quality at 1.5 and 3.0 Tesla magnetic resonance imaging. Eur Radiol 2009;19:1239–1245.
25. Schmid-Schwap M, Bristela M, Pittschieler E, et al. Biochemical analysis of the articular disc of the temporomandibular joint with magnetic resonance T2 mapping: A feasibility study. Clin Oral Investig 2014;18:1865–1871.
26. Goodwin DW, Wadghiri YZ, Zhu H, Vinton CJ, Smith ED, Dunn JF. Macroscopic structure of articular cartilage of the tibial plateau: Influence of a characteristic matrix architecture on MRI appearance. AJR Am J Roentgenol 2004;182:311–318.
27. Williams A, Gillis A, McKenzie C, et al. Glycosaminoglycan distribution in cartilage as determined by delayed gadolinium-enhanced MRI of cartilage (dGEMRIC): Potential clinical applications. AJR Am J Roentgenol 2004;182:167–172.
28. Trattnig S, Millington SA, Szomolanyi P, Marlovits S. MR imaging of osteochondral grafts and autologous chondrocyte implantation. Eur Radiol 2007;17:103–118.

29. Miller KL, Hargreaves BA, Gold GE, Pauly JM. Steady-state diffusion-weighted imaging of in vivo knee cartilage. Magn Reson Med 2004;51:394–398.
30. Welsch GH, Mamisch TC, Hughes T, Domayer S, Marlovits S, Trattnig S. Advanced morphological and biochemical magnetic resonance imaging of cartilage repair procedures in the knee joint at 3 Tesla. Semin Musculoskelet Radiol 2008;12:196–211.
31. Welsch GH, Mamisch TC, Hughes T, et al. In vivo biochemical 7.0 Tesla magnetic resonance: Preliminary results of dGEMRIC, zonal T2, and T2* mapping of articular cartilage. Invest Radiol 2008;43:619–626.
32. Mosher TJ, Dardzinski BJ. Cartilage MRI T2 relaxation time mapping: Overview and applications. Semin Musculoskelet Radiol 2004;8:355–368.
33. Trattnig S, Domayer S, Welsch GW, Mosher T, Eckstein F. MR imaging of cartilage and its repair in the knee—A review. Eur Radiol 2009;19:1582–1594.
34. Romeis B, Böck P. Mikroskopische Technik. Munich: Urban & Schwarzenberg, 1989.
35. Howard CV, Reid MG (eds). Estimation of component volume and volume fraction. In: Unbiased Stereology: Three-Dimensional Measurement in Microscopy. Oxford: BIOS Scientific, 1998: 55–68.
36. Gundersen HJ, Jensen EB. The efficiency of systematic sampling in stereology and its prediction. J Microsc 1987;147: 229–263.
37. Kochová P, Cimrman R, Janáček J, Witter K, Tonar Z. How to assess, visualize and compare the anisotropy of linear structures reconstructed from optical sections—A study based on histopathological quantification of human brain microvessels. J Theor Biol 2011;286:67–78.
38. Dryden IL, Koloydenko A, Zhou D. Non-euclidean statistics for covariance matrices, with applications to diffusion tensor imaging. Ann Appl Stat 2009;3:1102–1123.
39. Arsigny V, Fillard P, Pennec X, Ayache N. Geometric means in a novel vector space structure on symmetric positive-definite matrices. Siam J Matrix Anal Appl 2006;29:328–347.
40. Gründer W, Wagner M, Werner A. MR-microscopic visualization of anisotropic internal cartilage structures using the magic angle technique. Magn Reson Med 1998;39:376–382.
41. Nieminen MT, Rieppo J, Töyräs J, et al. T2 relaxation reveals spatial collagen architecture in articular cartilage: A comparative quantitative MRI and polarized light microscopic study. Magn Reson Med 2001;46:487–493.
42. Rubenstein JD, Kim JK, Morova-Protzner I, Stanchev PL, Henkelman RM. Effects of collagen orientation on MR imaging characteristics of bovine articular cartilage. Radiology 1993;188:219–226.
43. Fragonas E, Mlynárik V, Jellús V, et al. Correlation between biochemical composition and magnetic resonance appearance of articular cartilage. Osteoarthritis Cartilage 1998;6:24–32.
44. Xia Y. Heterogeneity of cartilage laminae in MR imaging. J Magn Reson Imaging 2000;11:686–693.
45. Kalpakci KN, Willard VP, Wong ME, Athanasiou KA. An interspecies comparison of the temporomandibular joint disc. J Dent Res 2011;90:193–198.